Journal of the European Ceramic Society 19 (1999) 837–841

PII: S0955-2219(98)00327-6
0955-2219/99/$ - see front matter

Lanthanide Co-doping of Solid Electrolytes: AC Conductivity Behaviour

J. van Herle,* D. Seneviratne and A. J. McEvoy

Ecole Polytechnique Fédérale de Lausanne, Departement Chimie, Laboratoire Photonique et Interfaces, 1015-Lausanne, Switzerland

Abstract

Solid electrolytes of cubic structure employed in Solid Oxide Fuel Cells (SOFC) like ceria (CeO_2) and zirconia (ZrO_2) are typically doped with a single selected element from the (Y, lanthanide)-series. Co-doping of ceria with several elements is investigated here in terms of its influence on ionic conductivity. It is found that, for a same total dopant concentration, mixtures of dopants give a higher total ionic conductivity (by 10–30%) than the best singly doped material. © *1999 Elsevier Science Limited. All rights reserved*

Keywords: co-doping, grain boundaries, ionic conductivity, CeO_2, fuel cells.

1 Introduction

Oxygen ion solid conductors are widely applied in fuel cells, sensors, separating membranes and other electrochemical devices. A high value of the ionic conductivity is obviously desirable for performance. In SOFC, the most widely used materials are cubic ZrO_2 and CeO_2 singly doped with yttrium or a lanthanide element. In this work, the effect of co-doping with several elements is investigated.

2 Experimental

Doped ceria powders were prepared by the oxalate route as previously reported.[1] All powders were compacted and sintered to 98% dense pellets at 1400°C for 4 h in air, to give similar microstructures, of which an example is given in Fig. 1.

*To whom correspondence should be addressed. Fax: +41-21-693-4111; e-mail:jan.vanherle@epfl.ch

The pellets were contacted on both sides, in a four-point setup, with silver wires and paint, transfered into a tubular oven and measured over 200–800°C in air. Measurements were carried out using electrochemical impedance spectroscopy (EIS, 10 mV, 1 MHz–0·1 Hz). Data were analyzed by equivalent electrical circuit fitting.

Compositions prepared and characterised so far are indicated in Table 1. The natural rare-earth mix used for sample '20RE' contained only the heavy lanthanides Sm through Lu. The 10CGO sample, the most widely used composition to date for a ceria electrolyte in real SOFC cells and stacks, served as a reference for comparison.

3 Theory

Following the analysis as described by Hohnke[2] or Kilner,[3] bulk ionic conduction in a solid electrolyte like doped ceria can be expressed as

$$\sigma_V T = \frac{A'}{W}.\exp(-(\Delta H_m + \Delta H_a))$$

at low temperature, and

$$\sigma_V T = A'.\frac{[\mathrm{LnO}_{1.5}]}{4}.\exp(-\Delta H_m)$$

at high temperature,

where ΔH_a is the defect association enthalpy, W the number of associate orientations (=4), $[\mathrm{LnO}_{1.5}]$ the lanthanide dopant concentration, and

$$A' = \frac{4e^2}{a_0 k}.\nu_0.\exp(\Delta S_m)$$

with a_0 as cubic lattice constant, ν_0 as lattice vibration frequency or vacancy jump attempt frequency and the subscript m referring to migration enthalpy and entropy, respectively.

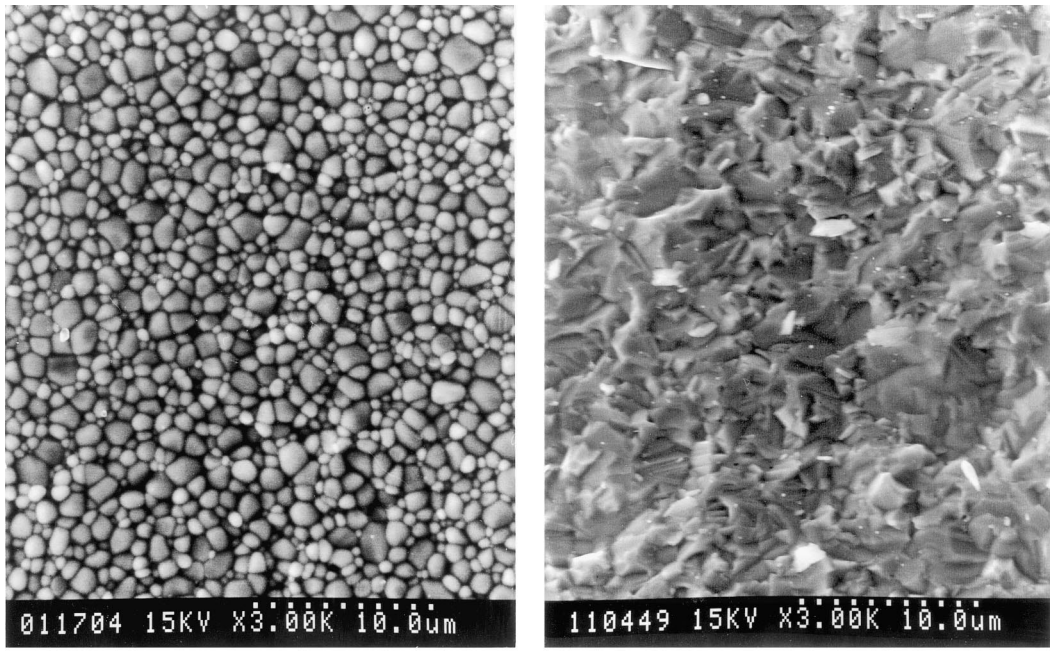

Fig. 1. (a) Surface view and (b) fracture view of a doped ceria pellet sintered at 1400°C for 4 h in air.

At intermediate temperatures, a gradual transition between the two activation energy limits, ΔH_m and $\Delta H_m + \Delta H_a$, appears as a curvature in the Arrhenius plot.

The derivation above is valid for dilute solid solutions up to approximately 15 mol% [$LnO_{1.5}$], the composition coinciding with maximal conductivity.[2,3]

Above this dopant concentration, the low temperature activation energy and preexponential factor increase with [$LnO_{1.5}$], the high temperature activation energy remaining constant.

4 Data Analysis

A typical resulting EIS of the samples is shown in Fig. 2. The high frequency response consisted of a single skewed arc, simulated by the combination of two R-CPE circuits, where the constant phase elements, $Z_{CPE} = 1/C(i\omega)^{\alpha}$, are interpreted as distributed capacitances. These can be arranged in four different ways (Fig. 3), giving all mathematically the exact same impedance, when assuming ideal capacitances ($\alpha_{CPE} = 1$).

The largest resistance R_g (= grain) of each circuit relates to the intragrain or bulk conductivity via

$$\sigma_V = \frac{1}{R_g} \cdot \frac{L}{A}$$

where L and A represent thickness and electrode area of the sample, respectively.

The popular bricklayer model as well as the third equivalent circuit shown in Fig. 3 are not considered here on the basis of arguments outside the scope of this paper. The 'blocking zone' model, as formulated by Bauerle,[4] describes the entire grain–grain contact not as consisting of a second,

Table 1. Compositions of mixed-doped ceria samples

Designation	*Composition*
10CGO	$(CeO_2)_{0.90}(GdO_{1.5})_{0.10}$
3×3GSY	$(CeO_2)_{0.91}(GdO_{1.5})_{0.03}(SmO_{1.5})_{0.03}(YO_{1.5})_{0.03}$
3×4GSY	$(CeO_2)_{0.88}(CdO_{1.5})_{0.04}(SmO_{1.5})_{0.04}(Y0_{1.5})_{0.04}$
3×5GSY	$(CeO_2)_{0.85}(GdO_{1.5})_{0.05}(SmO_{1.5})_{0.05}(YO_{1.5})_{0.05}$
3×6GSY	$(CeO_2)_{0.82}(GdO_{1.5})_{0.06}(SmO_{1.5})_{0.06}(YO_{1.5})_{0.06}$
5×2GSYND	$(CeO_2)_{0.90}(GdO_{1.5})_{0.02}(SmO_{1.5})_{0.02}(YO_{1.5})_{0.02}$ $(NdO_{1.5})_{0.02}(DyO_{1.5})_{0.02}$
5×3GSYND	$(CeO_2)_{0.85}(GdO_{1.5})_{0.03}(SmO_{1.5})_{0.03}(YO_{1.5})_{0.03}$ $(NdO_{1.5})_{0.03}(DyO_{1.5})_{0.03}$
20RE	$(CeO_2)_{0.80}(RE{-}O_{1.5})_{0.20}$

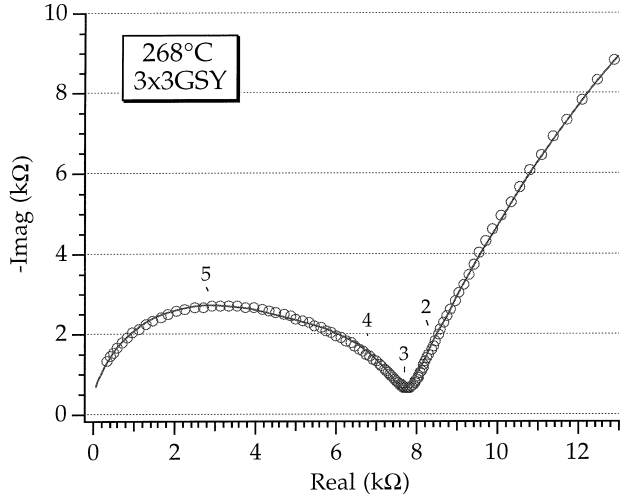

Fig. 2. EIS response of 3×3GSY pellet at 268°C. Numbers indicate frequencies in powers of 10 Hz.

separate glassy phase, but rather as an area where jumping of vacancies is slowed down. The 'constriction zone' model formulated by Schouler[5] defines the grain–grain contact as only partially blocked, R_g corresponding to the bulk conductivity multiplied with a tortuosity factor, and R_{gb} again as a zone where vacancy jumping is more difficult than within the grain.

We limit the analysis to the comparison between these blocking zone and constriction zone models, which essentially oppose a series resistive and parallel resistive network, respectively.

5 Discussion

Figure 4 shows the Arrhenius graph for the resulting bulk conductivities of a sample of 5×2GSYND, as derived from the serial and parallel circuit fits respectively. For both models, no kinks are apparent nor any other obvious deviations from

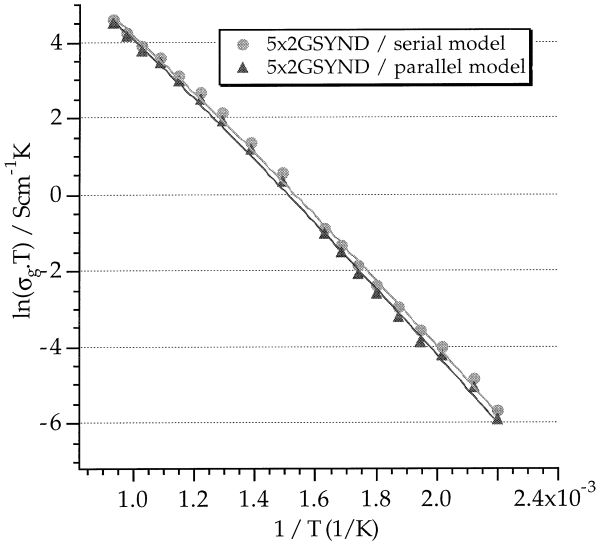

Fig. 4. Intragrain conductivity of a pellet with composition 5×2GSYND, as determined from both the blocking zone (serial resistive) and constriction zone (parallel resistive) models, respectively (see Fig. 3).

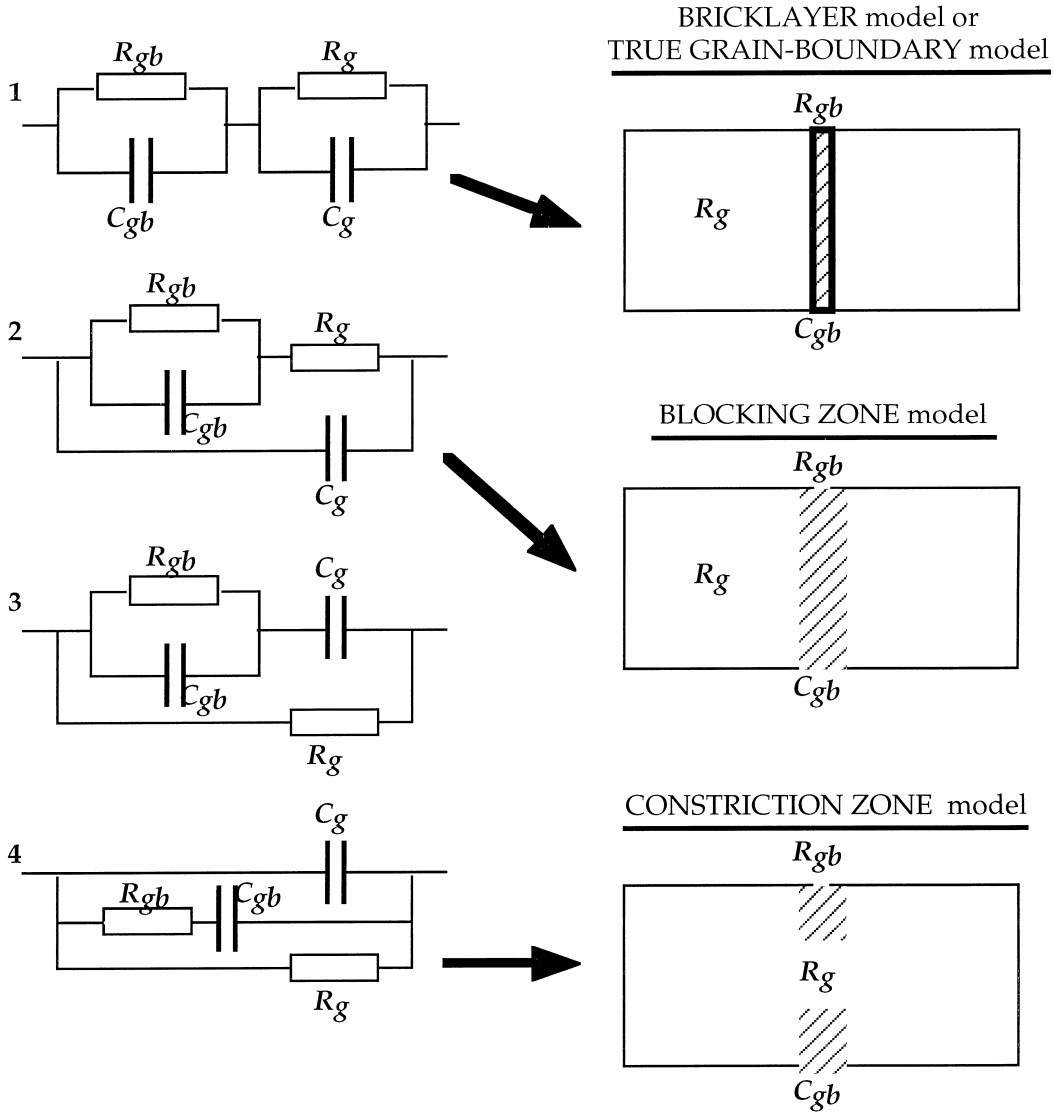

Fig. 3. Equivalent circuits used to fit the EIS response at low temperatures, with their corresponding physical models.

Table 2. Bulk conductivities σ_g ($S\,m^{-1}$) as determined from the serial resistive 'blocking zone' model (Fig. 3)

	10CGO	*3×3GSY*	*3×4GSY*	*5×2GSYND*	*5×3GSYND*	*3×5GSY*	*3×6GSY*	*20RE*
500°C	0·756	0·771	0·81	1·09	0·89	0·722	0·565	0·741
600°C	1·85	2·0	2·23	2·68	2·57	2·21	1·72	2·5
700°C	4·12	4·17	4·6	5·1	5·26	4·69	3·99	6·12
800°C	6·89	6·24	8·44	9·28	9·11	9·01	8·01	9·91
ΔH (eV)	0·618	0·544	0·617	0·575	0·588	0·655	0·716	0·643
ln A	11	10·1	11·21	10·8	11·0	11·6	12·2	11·7

Table 3. Bulk conductivities σ_g ($S\,m^{-1}$) as determined from the parallel resistive 'constriction zone' model (Fig. 3)

	10CGO	*3×3GSY*	*3×4GSY*	*5×2GSYND*	*5×3GSYND*	*3×5GSY*	*3×6GSY*	*20RE*	*20CGO*[a]	*20CSO*[a]	*20CYO*[a]
500°C	0·626	0·585	0·775	0·90	0·783	0·614	0·552	0·648	0·52	0·52	0·37
600°C	1·62	1·63	2·17	2·27	2·28	1·96	1·70	2·26	1·86	1·86	1·47
700°C	3·7	3·55	4·52	4·54	4·77	4·30	3·96	5·67	4·2	4·1	3·5
800°C	6·36	5·59	8·34	8·39	8·4	8·41	7·97	9·42	9·0	8·8	7·7
ΔH (eV)	0·638	0·584	0·623	0·596	0·602	0·675	0·719	0·663	0·751	0·744	0·795
ln A	11·2	10·4	11·2	10·9	11·0	11·8	12·2	12·0	12·4	12·2	12·6

[a]Rem: 20CGO, 20CSO and 20CYO refer to CeO_2 doped with 20 mol% $GdO_{1.5}$, $SmO_{1.5}$, and $YO_{1.5}$, respectively, the values of which were obtained from Ref. 7.

the expected behaviour, namely a straight line gradually curving into a lower slope at higher temperatures.[3] It follows that this testing criterion does not allow to favor one over the other model. Figure 4 allows to appreciate the influence of the 'grain boundary' contribution, which simply corresponds to the difference between the two curves. It appears that this contribution persists into higher temperatures, but becomes sufficiently small (10%) at temperatures of interest (500–800°C).

Absolute σ_g-values at these temperatures from both models for all compositions are tabulated in Tables 2 and 3. It strikes that 5×2GSYND shows a significantly higher conductivity (up to 30%) than the singly doped material with same dopant concentration, 10CGO. Gadolinium is known as the best dopant for ceria.[6] Sm-doped ceria nearly equals CGO, but Nd-, Dy- or Y-doped ceria are all worse conductors than CGO, giving higher defect association enthalpies than for the gadolinium case. It therefore surprises that a co-doped sample shows a lower activation energy and higher conductivity.

Within the series 3×3GSY, 3×4GSY, 3×5GSY and 3×6GSY, the composition 3×4GSY clearly indicates maximal conductivity (Tables 2 and 3). The composition 5×3GSYND, despite a 50% higher vacancy concentration, equals that of 5×2GSYND in conductivity terms (Tables 2 and 3). It therefore appears that for these co-doped samples, maximal conductivity is obtained for $[LnO_{1.5}] \approx 0{\cdot}10$–$0{\cdot}12$, which is lower than the accepted value of $[LnO_{1.5}] \approx 0{\cdot}15$–$0{\cdot}16$ for singly doped ceria.[2,3] Hence, equal or even higher conductivity is achieved by co-doping with a lower total dopant concentration than for single doping, offering the potential for lower materials cost.

Dopant concentrations above the ideal composition aggravate defect association, raising activation energy and lowering conductivity again, as evident for the series 3×3GSY through 3×6GSY in Tables 2 and 3. It is therefore surprising that the natural lanthanide mix Sm–Lu, at 20 cation% doping, gives the highest conductivity of all samples studied. Despite containing heavy lanthanides (activation energies increase from La to Lu-doping), the result in the natural mixture is such that the activation energy remains low (0·65 eV), indicating that defect associates break up at these temperatures and high dopant concentrations. The 20RE composition appears a better conductor (by about 20%) than singly doped ceria with the same vacancy concentration (Table 3).

Regarding the proposed theory for bulk ionic conduction in fluorites, activation energies and preexponential factors for bulk conductivities of all samples were investigated in more detail as a function of the vacancy concentration. This behaviour will be reported separately.

6 Conclusion

Co-doped ceria with three, five or 10 dopants shows significantly higher ionic conductivity in air (by 10–30%) than the best singly doped materials with the same vacancy concentration. The co-doped samples comply reasonably well with the theoretical model based on the defect associate equilibrium in terms of their conductivities. On the basis of equivalent electrical circuit fitting, no preference could be given to a serial or parallel arrangement of the two resistive contributions at low temperatures, corresponding to (i) the

dominant bulk resistivity and (ii) a resistance attributable to a partially or complete, but 'mild', blocking zone for vacancy jumping. The latter is probably only microstructure-related and unimportant at operating temperatures.

References

1. Van Herle, J., Horita, T., Kawada, T., Sakai, N., Yokokawa, H. and Dokiya, M., Sintering behaviour and ionic conductivity of yttria-doped ceria. *J. Eur. Ceram. Soc.*, 1996, **16**, 961–973.
2. Hohnke, D. K., Ionic conduction in doped oxides with the fluorite structure. *Solid State Ionics*, 1981, **5**, 531–534.
3. Kilner, J. A. and Waters, C. D., The effects of dopant cation–oxygen vacancy complexes on the anion transport properties of non-stoichiometric fluorite oxides. *Solid State Ionics*, 1982, **6**, 253–259.
4. Bauerle, J. E., Study of solid electrolyte polarization by a complex admittance method. *J. Phys. Chem. Solids*, 1969, **30**, 2657–2670.
5. Schouler, E., Giroud, G. and Kleitz, M., Applications selon Bauerle du tracé des diagrammes d'admittance complexe en électrochimie des solides II. *J. Chimie Physique*, 1973, **70**, 1309–1316.
6. Gerhardt-Anderson, R. and Nowick, A. S., Ionic conductivity of CeO_2 with trivalent dopants of different ionic radii. *Solid State Ionics*, 1981, **5**, 547–550.
7. Van Herle, J., Horita, T., Kawada, T., Sakai, N., Yokokawa, H. and Dokiya, M., Low temperature fabrication of (Y,Cd,Sm)-doped ceria electrolyte. *Solid State Ionics*, 1996, **86–88**, 1255–1258.